

IMAGING IN RADIO INTERFEROMETRY BY ITERATIVE SUBSET SCANNING USING A MODIFIED AMP ALGORITHM

*Giovanni Cherubini, Paul Hurley, Matthieu Simeoni, and Sanaz Kazemi**

IBM Research – Zurich, 8803 Rüschlikon, Switzerland

email: {cbi, pah, meo}@zurich.ibm.com

ABSTRACT

Imaging techniques in radio interferometry often face a significant challenge posed by the large number of antenna signals received, from which the image information needs to be extracted. Beamforming is envisaged to reduce the rate required for transporting data from groups of antennas to a central site for further processing. We propose a novel method for image reconstruction based on the iterative scanning of a region of interest, combined with randomized beamforming. A modified approximate message-passing algorithm is adopted to extract relevant image information from beamformed signals received at the antenna stations. The method is illustrated by simulations, with reference to the LOFAR radio interferometer, and compared with the CLEAN algorithm.

Index Terms— Radio interferometry, AMP algorithm, imaging, sensor arrays, antenna arrays

1. INTRODUCTION

Modern large-scale radio telescope arrays use antenna stations with multiple closely placed antennas for imaging the sky [1, 2]. The Square Kilometre Array (SKA), whose completion is expected within the next decade, will constitute the largest and most sensitive radio telescope ever built, consisting of several hundred thousand antennas for a total collection area of 1 km². The challenge posed by the sheer amount of data collected, on the order of several tens of Terabits per second, is enormous. To reduce the amount of data to be transported from the stations to a central site for further processing, the signals received by the antennas at a station are combined by beamforming. Typically, conjugate matched beamforming towards the center of the field of view is applied at all antenna stations. Random beamforming techniques were also proposed [3]. The beamformed signals from all stations are correlated to obtain so-called visibilities, which are related to the samples of the Fourier transform of the sky image [4]. Several deconvolution algorithms were proposed for reconstructing the sky image based on the inverse Fourier transform of the entire collection of visibility measurements [5]–[9].

In imaging applications for radio astronomy, the pixelated region of interest often entails a large number of elements, especially in the case of high-resolution images. For example, sky images with as many as 10⁸ pixels are required for specific astronomical investigations [10]. In such cases, the complexity of implementing image-reconstruction algorithms becomes very challenging. It is therefore essential to devise methods that combine the efficiency and the convergence properties of low-complexity algorithms with a substantial reduction of the memory and computational requirements for image reconstruction with a desired resolution.

We propose a novel method for image reconstruction in sensor array systems, based on the iterative scanning of a region of interest, combined with randomized beamforming. The method is applied in the time domain, rather than in the frequency domain as the state-of-the-art approaches mentioned above. It is well suited to capture fast transient phenomena, as it can extract image information from short observation intervals. Scanning is achieved by subdividing the region of interest into subsets of points on a grid, and extracting information about point source intensities from each subset. The overall image is reconstructed by combining the information recovered from each subset.

A modified approximate message passing (AMP) algorithm over a factor graph connecting hypothetical source intensity nodes and measurement nodes is used to recover, with low computational effort, the intensities associated with sources located at the points of each subset. The steps of randomization and pruning are introduced to obtain satisfactory results in the case of significant deviations from a Gaussian distribution of the matrix elements that relate source and measurement nodes. The AMP algorithm was recently proposed as an efficient implementation of the sum-product algorithm on factor graphs [11, 12]. It has the attractive feature of allowing an equivalent formulation as an iterative thresholding algorithm [13], thus providing the reconstruction power of l_1 minimization techniques when sparsity of the solution can be assumed, as is often the case in radio interferometry [14]. The proposed method can be applied for image reconstruction in general in systems where no beamforming is applied to recover image information from sensor signals [15]. Here we focus on imaging for radio astronomy applications.

*Work performed while with IBM Netherlands.

This work was supported in part by the Province of Drenthe, Netherlands, and the Dutch Ministry of Economic Affairs.

2. RADIO INTERFEROMETRY SYSTEM MODEL

Consider a radio interferometer with L antenna stations, where the i -th station comprises L_i antennas with positions given by $\mathbf{p}_j^{(i)}$, $j = 1, \dots, L_i$, and one beamforming matrix, see Fig. 1. The antennas receive narrow-band signals centered at the frequency f_0 . The signal received at the i -th antenna station at time k from a source s_q in a direction identified by the unit vector $\mathbf{r}_{q,k}$ is expressed as

$$\mathbf{x}_{q,k}^{(i)} = \mathbf{a}^{(i)}(\mathbf{r}_{q,k}) s_q, \quad (1)$$

where $\mathbf{a}^{(i)}(\mathbf{r}_{q,k})$ is the $L_i \times 1$ antenna array steering vector for the i -th station and direction $\mathbf{r}_{q,k}$, given by

$$\mathbf{a}^{(i)}(\mathbf{r}_{q,k}) = \left(e^{-j2\pi\langle \mathbf{p}_1^{(i)}, \mathbf{r}_{q,k} \rangle}, \dots, e^{-j2\pi\langle \mathbf{p}_{L_i}^{(i)}, \mathbf{r}_{q,k} \rangle} \right)^T, \quad (2)$$

where $\langle \mathbf{p}, \mathbf{r} \rangle$ denotes the inner product between the vectors \mathbf{p} and \mathbf{r} , and \mathbf{x}^T is the transpose of \mathbf{x} . Assuming there are Q point sources in the sky, the overall noisy signal received at the i -th antenna station after beamforming is expressed as

$$\mathbf{x}_{b,k}^{(i)} = \mathbf{W}^{(i)H} \mathbf{x}_k^{(i)} = \mathbf{W}^{(i)H} \left(\mathbf{A}_k^{(i)} \mathbf{s}_q + \boldsymbol{\eta}_k^{(i)} \right), \quad (3)$$

where the complex vector \mathbf{s}_q denotes the signals emitted by the sources; matrix $\mathbf{A}_k^{(i)}$ is formed by the column vectors $\mathbf{a}^{(i)}(\mathbf{r}_{q,k})$, $q = 1, \dots, Q$; $\boldsymbol{\eta}_k^{(i)}$ denotes the noise vector at the i -th antenna station, and $\mathbf{W}^{(i)H}$ is the conjugate transpose of the beamforming matrix $\mathbf{W}^{(i)}$. The expected value of the correlator output that uses the beamformed signals from the L stations to produce the visibilities for image reconstruction is given by

$$\mathbf{R}_k = \begin{pmatrix} \mathbf{R}_k^{(1,1)} & \mathbf{R}_k^{(1,2)} & \dots \\ \vdots & \ddots & \vdots \\ \mathbf{R}_k^{(L,1)} & \dots & \mathbf{R}_k^{(L,L)} \end{pmatrix}, \quad (4)$$

where

$$\mathbf{R}_k^{(i,j)} = \mathbf{W}^{i(H)} \left(\mathbf{A}_k^{(i)} \boldsymbol{\Sigma}_s \mathbf{A}_k^{(j)H} + \boldsymbol{\Sigma}_\eta^{(i,j)} \right) \mathbf{W}^{(j)}, \quad (5)$$

and where, assuming independent Gaussian sources and independent Gaussian antenna noise signals, the correlation matrix of the signals emitted by the sources $\boldsymbol{\Sigma}_s$ is a diagonal matrix, and the correlation matrix of the noise signals $\boldsymbol{\Sigma}_\eta^{(i,j)}$ is a nonzero diagonal matrix for $i = j$, and a zero $L_i \times L_j$ matrix otherwise.

Observing (5), it turns out that each element in $\mathbf{R}_k^{(i,j)}$ can be expressed as a linear combination of the source intensities σ_q^2 found in the diagonal of $\boldsymbol{\Sigma}_s$, plus measurement noise. In practice, an estimate of \mathbf{R}_k is obtained from a finite number of samples. Therefore an additional disturbance needs to be taken into account that arises from the deviation from the ideal values of the correlation matrix estimates of both the source intensities $\hat{\boldsymbol{\Sigma}}_s$ and the antenna noise signals $\hat{\boldsymbol{\Sigma}}_\eta^{(i,i)}$.

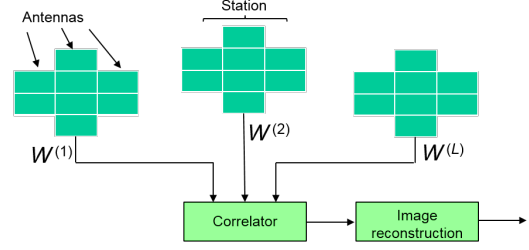


Fig. 1. Block diagram of a radio interferometer

For image reconstruction, the region of interest is subdivided into a collection of hypothetical intensity sources at arbitrary positions, corresponding to the N points on a 2D grid. For a single source with unit intensity at the k -th point in the grid, i.e., $\sigma_k^2 = 1$ and $\sigma_j^2 = 0$ for $j \neq k$, the signal received at the correlator output is obtained in the ideal case by (4) and (5), with $\boldsymbol{\Sigma}_s = \text{diag}(0, \dots, 0, \sigma_k^2 = 1, 0, \dots, 0)$ and $\boldsymbol{\Sigma}_\eta^{(i,i)} = 0$. The antenna steering vectors forming the columns of $\mathbf{A}_k^{(i)}$ are computed by considering the N direction vectors defined by the points in the grid. After the received signals for all hypothetical unit sources in the grid have been determined, and considering the Hermitian symmetry of the correlation matrix, the responses obtained are reshaped to form a matrix \mathbf{V}_k , with the number of rows given by $M = M'L(M'L + 1)/2$, assuming M' beamforms are used at each of the L stations. Recalling that in radio interferometry the correlation samples, also known as visibilities, are collected over K short-term integration (STI) intervals and that the antenna steering vectors may be considered constant within one STI, but are time varying in general, the observation model then becomes

$$\begin{pmatrix} \rho_1 \\ \rho_2 \\ \vdots \\ \rho_K \end{pmatrix} = \begin{pmatrix} \mathbf{V}_1 \\ \mathbf{V}_2 \\ \vdots \\ \mathbf{V}_K \end{pmatrix} \mathbf{s} + \begin{pmatrix} \tilde{\eta}_1 \\ \tilde{\eta}_2 \\ \vdots \\ \tilde{\eta}_K \end{pmatrix}, \quad (6)$$

where for the k -th STI ρ_k denotes the vector of correlation samples; \mathbf{V}_k is the matrix of responses of hypothetical point sources with unit intensity on the assumed grid; $\tilde{\eta}_k$ is a vector of measurement noise terms, and \mathbf{s} is the vector of hypothetical point source intensities.

3. ITERATIVE IMAGE SUBSET SCANNING METHOD

The proposed imaging method is based on the iterative scanning of a fine grid \mathfrak{S} defined over the region of interest. At the j -th iteration, scanning is achieved by subdividing the points of the grid into subsets, not necessarily uniform or disjoint, which belong to a set $\mathfrak{S}^{(j)} \subseteq \mathfrak{S}$, and extracting information about point source intensities in each subset. With reference to the radio interferometry system model of Sec. 2, the observation of the hypothetical sources located at the i -th subset of points on the grid, $\Omega(i, j) \subset \mathfrak{S}^{(j)}$, $i = 1, \dots, |\mathfrak{S}^{(j)}|$, where

$|\mathfrak{S}^{(j)}|$ denotes the cardinality of $\mathfrak{S}^{(j)}$, is expressed as

$$\begin{pmatrix} \rho_1 \\ \rho_2 \\ \vdots \\ \rho_K \end{pmatrix} = \begin{pmatrix} \mathbf{V}_1^{(i,j)} \\ \mathbf{V}_2^{(i,j)} \\ \vdots \\ \mathbf{V}_K^{(i,j)} \end{pmatrix} \mathbf{s}^{(i,j)} + \begin{pmatrix} \tilde{\eta}_1^{(i,j)} \\ \tilde{\eta}_2^{(i,j)} \\ \vdots \\ \tilde{\eta}_K^{(i,j)} \end{pmatrix}, \quad (7)$$

where the vector $\mathbf{s}^{(i,j)}$ denotes the hypothetical point source intensities in $\Omega(i, j)$, and the subsets satisfy the condition

$$\bigcup_{i=1, \dots, |\mathfrak{S}^{(j)}|} \Omega(i, j) = \mathfrak{S}^{(j)}, \quad \forall j. \quad (8)$$

For fixed i and j , there is a one-to-one correspondence between the elements of the vector $\mathbf{s}^{(i,j)}$ and the elements of the set of direction vectors $\{\mathbf{r}_n^{(i,j)}\}_{n=1}^{|\Omega(i,j)|}$, defined by the i -th subset of points on the grid at the j -th iteration. Beamforming matrices $\mathbf{W}^{(l)}$, $l = 1, \dots, L$, are applied to match M_l columns of the antenna steering matrices $\mathbf{A}_k^{(l,i,j)}$, where the index l identifies the l -th station. The beamforming matrix $\mathbf{W}^{(l)}$ is formed by randomly selecting M_l columns from the antenna steering matrix, without repetition of the direction vectors, i.e., by matched beamforming towards randomly chosen directions within the region of interest [3].

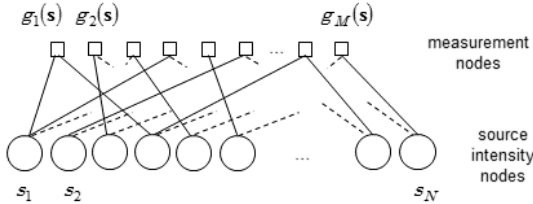


Fig. 2. Block diagram of a fully connected factor graph.

A modified AMP algorithm is applied over the factor graph of Fig. 2 to estimate the point source intensities in each subset, where the variable nodes are the source intensities and the function nodes represent the measurements obtained from the correlation samples over K STI intervals as expressed in (7). To further reduce memory and computational requirements, the measurements obtained by one STI interval at a time are considered for message passing. Let us consider applying the AMP algorithm to extract information about the hypothetical source intensities at the points in the i -th subset during the j -th scanning iteration, $\Omega(i, j)$, at the k -th STI interval. The prior probability of the source intensities at the first STI interval is assumed to have a Bernoulli–Log Normal distribution. When the AMP algorithm at the k -th STI interval terminates, the estimates obtained are used to define a new prior with a Gaussian distribution for the application of the algorithm within the $(k + 1)$ -th STI interval. The procedure continues over the K STI intervals, leading to the final estimate of $\mathbf{s}^{(i,j)}$.

As shown in [11], the AMP algorithm yields the true posterior means, in the limit $M, N \rightarrow \infty$, provided the ratio M/N is fixed, and assuming the elements of $\mathbf{V}_k^{(i,j)}$ are i.i.d.

Gaussian random variables. In practice, however, the number of both the source intensity nodes N and the measurements nodes M are finite, and the elements of $\mathbf{V}_k^{(i,j)}$ may deviate significantly from a Gaussian distribution. Therefore, the following two modifications of the AMP algorithm are introduced to obviate those limitations:

1. Randomization. The factor graph of Fig. 2 is fully connected and hence exhibits a large number of short cycles, leading to a non-negligible estimation error. This effect is mitigated by a random permutation of the measurement nodes at the end of each iteration of the AMP algorithm.

2. Pruning. In the applications considered, the condition $M \gg N$ is usually satisfied, hence sufficient flow of information within the factor graph is achieved if some of the messages passed from the measurement nodes to the source nodes are pruned. Thereby only a subset of the messages will be considered for the computation of the estimate of $\mathbf{s}^{(i,j)}$, such that the distribution of the elements of $\mathbf{V}_k^{(i,j)}$, which correspond to the allowed connections in the factor graph, is approximately Gaussian.

The modified AMP algorithm is applied to obtain estimates $\{\hat{\mathbf{s}}_K^{(i,j)}, \dots, \hat{\mathbf{s}}_K^{(|\mathfrak{S}^{(j)}|, j)}\}$ at the j -th scanning iteration.

An estimate of the vector $\hat{\mathbf{s}}_K^{(j)}$ of the intensities of hypothetical sources located on the points of the entire grid is obtained by combining the information recovered from each subset. The detection of sources at points of the grid may be obtained by a threshold operation on the elements of the vector $\hat{\mathbf{s}}_K^{(j)}$. At the $(j + 1)$ -th iteration, the subsets $\Omega(i, j + 1)$ are modified with respect to the subsets defined at the j -th iteration to achieve two goals: First, a subset is extended with points corresponding to sources identified in the preceding iteration to reduce the level of background clutter. Second, one or more subsets may be defined on a finer grid to achieve a better image resolution in a portion of the region of interest, provided the location and number of antenna stations allow a higher resolution. After a predefined number J of iterations of the scanning beamforming method has been completed or a desired accuracy has been achieved in the estimate of the source intensities, the process terminates.

4. PERFORMANCE ANALYSIS

Now we present numerical simulation showing the effectiveness of our iterative image subset scanning method combined with randomized beamforming. A radio interferometry system with 24 antenna stations having 48 antennas each is considered. Its geographical distribution corresponds to the locations of the LOFAR array [1]. In the simulations, a field of view of 0.02 rad radius is assumed. In it, six point sources are found, with intensities having a Rayleigh distribution with variance $(\pi/2)^{1/2} \sim 1.25$. Correlation of the received antenna signals is performed over 768 samples within an STI interval of 1 s, which corresponds to $K = 1$ in (7). To apply the proposed method, the field of view is subdivided into a

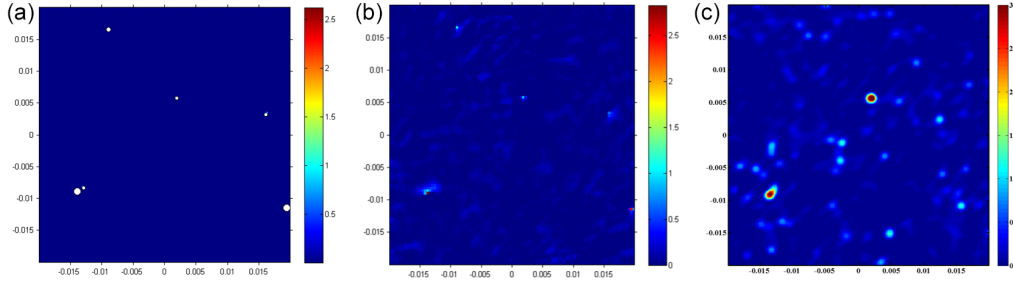


Fig. 3. (a) Target sky, (b) reconstructed sky after three iterations of the proposed method, and (c) reconstructed sky by the CLEAN algorithm.

collection of hypothetical intensity sources at arbitrary positions corresponding to uniformly distributed points within a 100×100 grid.

The scanning of the field of view takes place over 100 subsets, i.e., $|\mathcal{S}^{(j)}| = 100$ for all j . At the first scanning iteration, the subsets are uniformly chosen within the 100×100 grid, i.e., the points in each subset are uniformly distributed over a 10×10 grid, with a minimum distance between points of $10 \times$ the minimum distance between points in the fine grid. The estimation of the source intensities for the points of each subset is achieved by 32 iterations of the modified AMP algorithm described in Sec. 3, including the random permutation of the measurement nodes at the end of each message-passing iteration. Pruning of selected messages passed from the measurement nodes to the variable nodes is also adopted to approximate a Gaussian distribution of the elements of the matrix $\mathbf{V}_1^{(i,j)}$. Thereby a message from a measurement node to a variable node is pruned if the following condition on the (m, n) -th element of $\mathbf{V}_1^{(i,j)}$ is not satisfied:

$$\text{Re} \left\{ v_{1,m,n}^{(i,j)} \right\} < 0.1 \wedge \text{Im} \left\{ v_{1,m,n}^{(i,j)} \right\} > -0.1. \quad (9)$$

The approximation achieved by applying the above condition is illustrated in Figs. 4 and 5, showing the distributions of the real and imaginary part of all coefficients of $\mathbf{V}_1^{(1,1)}$ and of those retained after pruning the graph.

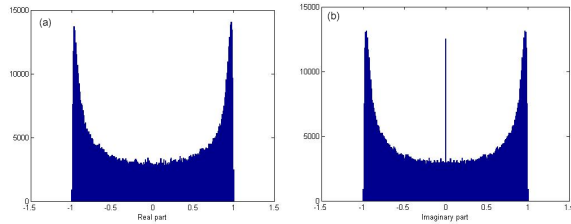


Fig. 4. Distribution of (a) real and (b) imaginary part of $\mathbf{V}_1^{(1,1)}$ elements.

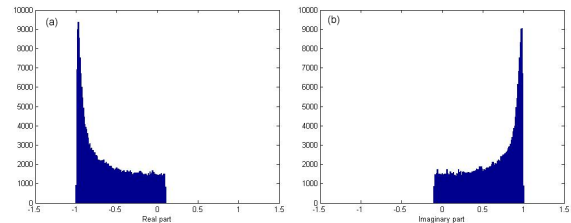


Fig. 5. Distribution of the (a) real and (b) imaginary part of $\mathbf{V}_1^{(1,1)}$ elements retained after pruning the graph for the modified AMP.

Let us consider a reconstructed image obtained after three scanning iterations. A measure of the image quality after the j -th iteration is given by the following metric, which represents a measure of the residual error:

$$e_{\text{res}}^{(j)} = \sqrt{\frac{\sum_{n=1}^N (\hat{s}_n^{(j)} - s_n)^2}{N}}, \quad (10)$$

where $\hat{s}_n^{(j)}$ denotes the estimated intensity at point n in the fine grid after iteration j . Figure 6 shows the residual error versus the SNR, defined as $10 \log((\pi/2)^{1/2}/\sigma_\eta^2)$, for the first three iterations. Threshold detection is applied at the end of each iteration to identify the strongest sources, with a variable threshold set at about one half of the highest intensity after the first iteration and divided by two after each further iteration. After detection, each subset is augmented by the points corresponding to the detected sources to reduce the clutter. Figure 3(a) shows the target sky and 3(b) the reconstructed image after three iterations for an SNR of -18 dB. For comparison, Fig. 3(c) shows the image obtained by the CLEAN algorithm [4], based on the Fourier transform of the same set of visibilities as used to generate the image in Fig. 3(b).

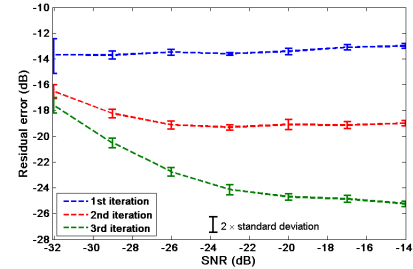


Fig. 6. Residual error vs. SNR for the sky of Fig. 3(a).

5. CONCLUSION

We presented a new image reconstruction method and introduced the concept of iterative scanning of a region of interest subdivided into subsets combined with randomized beamforming, together with a modified AMP algorithm for efficient extraction of relevant image information from signals received by sensor arrays. Simulation results obtained with reference to the LOFAR interferometer indicate that the proposed method yields significantly more accurate image reconstruction for short observation intervals than the CLEAN deconvolution algorithm.

6. REFERENCES

- [1] M. de Vos, A. W. Gunst, and R. Nijboer, "The LOFAR telescope: System architecture and signal processing," *Proc. IEEE*, vol. 97, no. 8, pp. 1431-1437, Aug. 2009.
- [2] P. E. Dewdney, P. J. Hall, R. T. Schilizzi, and T. J. L. W. Lazio, "The Square Kilometre Array," *Proc. IEEE*, vol. 97, no. 8, pp. 1482-1496, Aug. 2009.
- [3] O. Ocal, P. Hurley, G. Cherubini, and S. Kazemi, "Collaborative randomized beamforming for phased array radio interferometers," *Proc. 40th IEEE Int'l Conf. on Acoustics, Speech, and Signal Processing, ICASSP 2015*, Brisbane, Australia, Apr. 2015, pp. 5654-5658.
- [4] A. J. van der Veen and S. J. Wijnholds, "Signal processing tools for radio astronomy," in: *Handbook of Signal Processing Systems*, 2nd ed., Springer, May 2013.
- [5] J. A. Högbom, "Aperture synthesis with a non-regular distribution of interferometer baselines," *Astronomy and Astrophysics*, vol. 15, p. 417, Jun. 1974.
- [6] U. Rau and T. J. Cornwell, "A multi-scale multi-frequency deconvolution algorithm for synthesis imaging in radio interferometry," *Astronomy and Astrophysics*, vol. 532, article A71, Aug. 2011.
- [7] P. M. Sutter, B. D. Wandelt, J. D. McEwen, E. F. Bunn, A. Karakci, A. Korotkov, P. Timbie, G. S. Tucker, and L. Zhang, "Probabilistic image reconstruction for radio interferometers," *MNRAS*, vol. 438, pp. 768-778, Feb. 2014.
- [8] C. Tasse, S. van der Tol, J. van Zwieten, G. van Diepen, and S. Bhatnagar, "Applying full polarization A-Projection to very wide field of view instruments: An imager for LOFAR," *Astronomy and Astrophysics*, vol. 553, article A105, May 2013.
- [9] T. J. Cornwell, K. Golap, and S. Bhatnagar, "The non-coplanar baselines effect in radio interferometry: The W-projection algorithm," *IEEE J. Sel. Topics in Signal Processing*, vol. 2, no. 5, pp. 647-657, Nov. 2008.
- [10] M. W. Powell, R. Rossi, and K. Shams, "A scalable image processing framework for gigapixel Mars and other celestial body images," *Proc. 2010 IEEE Aerospace Conference*, pp. 1-11, 2010.
- [11] M. Bayati and A. Montanari, "The dynamics of message passing on dense graphs, with applications to compressed sensing," *IEEE Trans. Information Theory*, vol. 57, no. 2, pp. 764-785, Feb. 2011.
- [12] S. Som and P. Schniter, "Compressive imaging using approximate message passing and a Markov-tree prior," *IEEE Trans. Signal Processing*, vol. 60, no. 7, pp. 3439-3448, Jul. 2012.
- [13] P. R. Gill, A. Wang, and A. Molnar, "The in-crowd algorithm for fast basis pursuit denoising," *IEEE Trans. Signal Processing*, vol. 59, no. 10, pp. 4595-4605, Oct. 2011.
- [14] H. Garsden, *et al.*, "LOFAR sparse image reconstruction," *Astronomy and Astrophysics*, vol. 575, article A90, Mar. 2015.
- [15] G. Cherubini, P. Hurley, M. Simeoni, and S. Kazemi, "Iterative Image subset scanning for image reconstruction from sensor signals," *Proc. 15th IEEE Int'l Symposium on Signal Processing and Information Technology, ISSPIT 2015*, Abu Dhabi, UAE, Dec. 2015, pp. 602-607.